Development and Evaluation of Soft Headforms Representing Japanese Facial Features for Improved Respirator Fit Testing

Hiroki Haruta*, Hisashi Yuasa

Koken LTD., Basic Laboratory, 3-10-1 Akanedai, Hanno, Saitama, 357-0044, Japan.

* Corresponding author email: haruta@koken-ltd.co.jp

ABSTRACT

Introduction: Respirator fit is significantly impacted by facial features, which can differ greatly due to the diversity in race and ethnicity. In our previous study, we reported on a PCA panel for Japanese workers (Haruta et al., 2023) that better represented the Japanese facial features, along with five corresponding digital headforms.

Objective: This report describes the construction of digital headforms into “soft headforms” with softness and elasticity parameters similar to a human face, and evaluates their respirator fit.

Methods: Using a skin softness and elasticity meter, the skin deformation curves at 10 facial points on each subject were measured to obtain softness and elasticity parameters. Based on the information obtained from the subject test, five soft headforms were developed using an elastic material. Finally, the fit factors of the soft headforms for the six respirator models were compared with those of hard headforms (plastic) with identical dimensions.

Results: In the subject test, the softness parameter values varied across various points, including the cheek and chin, whereas the elasticity parameter values were almost constant, regardless of the points. The softness and elasticity parameters of the five soft headforms were also measured, confirming that most values fell within the target ranges determined from the subject test. For the fit factor evaluation, while the geometric mean fit factors of all respirator models on hard headforms were below 100, soft headforms could achieve 100 or more, depending on the combination of headform type and respirator model.

Conclusions: The soft headforms had higher fit factors, confirming the efficacy of elastic material in improving respirator fit. However, further research is required to assess the effect of headform type and respirator model on fit factors by comparing subject groups in the corresponding facial category in the Specified PCA panel for Japanese workers.

Keywords: respiratory protection, respirator fit, headform, elastic material, facial features, skin deformation

INTRODUCTION

Respirator fit is important for ensuring respiratory protection for respirator wearers, as residual face seal leakage is a major factor allowing a large number of harmful particles to leak into a facepiece (Myers, 2000; Grinshpun et al., 2009). Respirator fit is reportedly significantly affected by facial size and shape (Oestenstad et al., 1990; Groce et al., 2010). In the US, the NIOSH-bivariate panel using two facial dimensions and the NIOSH-PCA panel using ten facial and head dimensions were developed as new test panels based on survey facial data of the modern US workforce population (Zhuang and Bradmiller, 2005; Zhuang et al., 2007), replacing the traditional Los Alamos panel (Hack et al., 1974). The NIOSH-PCA panel has five facial categories (Small, Medium, Large, Short-Wide, and Long-Narrow) based on overall face size and shape. The corresponding headforms for the five facial categories in the panel were further created as 3D digital models (Zhuang et al., 2010) and adopted by the International Organization for Standardization

（ISO）for respirator performance testing (ISO, 2022). Since the headform models corresponding to the NIOSH-PCA panel were based on facial dimension data in the US, the development of 3D digital models in different shapes based on the facial and head dimensions of the working population in other countries with different facial shape characteristics has been reported. Yu et al. (2012) developed five digital headforms representing Chinese workers using anthropometric data obtained from Chinese workers, and reported that the developed medium headform differed in facial features from the NIOSH medium headform. Lee et al. (2024) further developed a set of five types of headforms reflecting the features of Korean faces and heads to evaluate the performance of respirators. The facial features of US and Japanese workers also differ according to their racial and ethnic diversity. In our previous study, we developed a Specified PCA panel for Japanese workers that better represented Japanese facial features (Haruta et al., 2016). Additionally, using 3D scan data of Japanese subjects and a homologous modeling technique, we developed five digital models corresponding to the five facial categories in the panel (Haruta et al., 2023).

The material used for headforms is also important for converting digital models into testable headforms for respirator fit testing. In prior studies, respirator fit evaluations of half-face respirators using conventional headforms made of materials stiffer or thinner than the human facial skin, such as rubber-coated, plastic, or compressible materials, have reported high leakage rates (Cooper et al., 1983; Tuomi, 1985; Golshahi et al., 2013).

Due to the challenges in achieving a proper face seal with conventional headforms, respirators sealed onto headforms with artificially-adjusted leak sites have been used to measure leakages within respirators (Hinds and Kraske, 1987; Rengasamy and Eimer, 2011). However, artificial leak sites may not accurately represent the actual conditions experienced by individuals wearing respirators (Krishnan et al., 1994).

Studies on headforms made from silicone materials that closely resemble the human skin for evaluating respirator fit have been reported. In one such study, Joe et al. (2012) fabricated five types of NIOSH headforms for respirator fit testing using commercially available flexible silicone materials. They conducted fit evaluations using a negative-pressure fit tester on three respirator models in a three-size system. They found that only combinations of two sizes in one respirator model and the short-wide headform achieved measurable negative pressure conditions, while other combinations were not measurable, suggesting that different formulations of silicone or other elastic materials might be required to conduct appropriate fit testing using headforms. NIOSH also developed an advanced headform, which is the NIOSH medium headform, using a novel elastic material that mimics the softness and thickness of human facial skin. Respirator fit testing for seven respirator models was conducted under two cyclic flow conditions. Compared to studies using older headforms constructed of conventional materials, the advanced headform significantly reduced leakage from the face seal, and achieved higher fit factors (Bergman et al., 2014). Moreover, For eight respirator models, a statistically significant correlation was observed between the mean log-transformed fit factors of ten subjects, including seven subjects categorized as medium in the NIOSH-PCA panel, and the medium-advanced headform (Bergman et al., 2015).

Such headforms capable of accurately assessing respirator fit are not only valuable in the design and development of better respirators, but also in the investigation of the practical performance of respirators for actual hazardous substances, for which it is unfeasible to conduct fit tests on human subjects. He et al. (2014) previously investigated the total inward leakages of paper, wood, and plastic combustion aerosols using the medium-advanced headform equipped with one type of respirator with a P100-class filter under three cyclic breathing flow rates and five breathing frequencies. They found that both the breathing flow rate and the type of combustion aerosol had a significant effect on the total inward leakage.

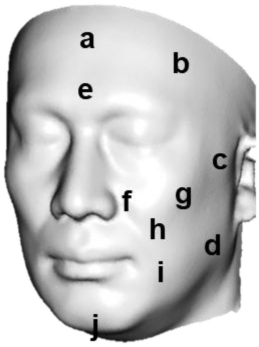
In contemporary Japan, national standards pertaining to respirator performances involve measuring the increase in carbon dioxide concentration within a facepiece (to assess dead space within the facepiece) and evaluating leakage rates for powered air-purifying respirators, which are conducted using a standardized test headform (Ministry of Health, Labor, and Welfare, 1963 and 2016). This standardized test headform in Japan comes in only one type, a rigid plastic “Hard-headform,” and is thus limited by the same issue of poor respirator fit observed in past studies using conventional headforms.

The objective of this study aimed to develop and evaluate soft headforms that represent Japanese facial features and can be used to improve to respirator fit testing. We initially investigated the physical properties of the facial skin of Japanese subjects using a skin softness and elasticity measuring device widely used in the medical and cosmetic fields. Using the obtained data as a reference, we materialized the five digital models corresponding to the facial categories in the Specified PCA panel for Japanese workers (Haruta et al. 2023) into five testable headforms with elastic materials referred to as “soft headform.” The performance of the respirator fit for the soft headforms was evaluated through comparison with plastic headforms (hard headforms) of identical dimensions.

METHODS

Measurement of softness and elasticity parameters on subject faces

The skin deformation curves were measured on the faces of thirty-one healthy adult subjects, aged 22–65 years, using a noninvasive skin softness and elasticity measurement device (MPA580, Courage + Khazaka Electronic GmbH, Cologne). Although the subjects were not selected based on facial type category, classification according to the previously defined PCA panel indicated that six subjects were in the Small category, 17 in Medium, three in Large, three in Short-Wide, and two in Long-Narrow. In this study, the measurements were conducted without considering facial category.



a. Forehead region
b. Frontotemporal region
c. Zygion
d. Gonion
e. Glabella
f. Nose side
g. Cheek region 1 (on zygomatic bone)
h. Cheek region 2
i. Cheek region 3
j. Chin

Figure 1. Measurement points on a face.

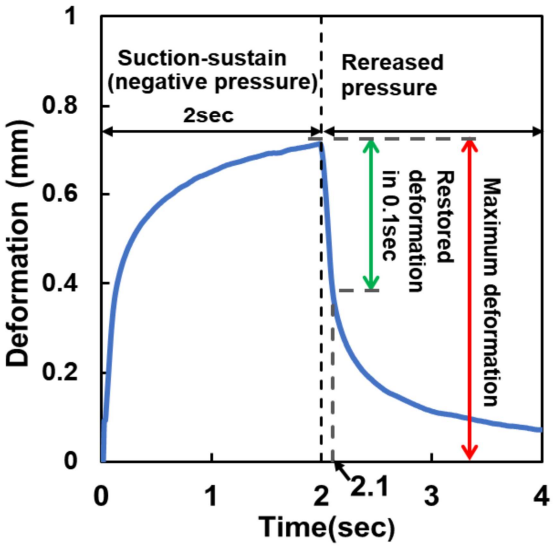


Figure 2. An example skin deformation curve and parameters.

Parameters related to softness and elasticity were subsequently calculated from the obtained skin deformation curves. The study design was approved by the Koken institutional review board. The number of measurement points on the subjects’ s faces was set to ten, as presented in Figure 1, including points considered to affect respirator fit. The device used in this study is widely used in both the medical and cosmetic fields (Courage + Khazaka Electronic GmbH. Abstracts Cutometer, 2024). To briefly describe the measurement using this device, a probe was applied to the target skin, which was suctioned using negative pressure. After a certain period, the negative pressure was released. A deformation curve showing skin deformation over time was obtained, as presented in Figure 2. By analyzing the deformation curve, parameters indicative of various physical properties of the skin can be derived. This study focused on skin softness and elasticity as properties potentially affecting respirator fit. Based on the technical

documentation of the device (Courage + Khazaka electronic GmbH Instruction Manual, 2013) and previous studies that measured subjects' facial properties using the same device (Akhtar et al., 2011; Kawabata et al., 2012), the measurement condition for suction and holding times were set to 2 seconds, the maximum amount of deformation during decompression was determined from the deformation curve, and used as a parameter to indicate skin softness. The ratio of the recovered deformation (0.1 s after decompression release) to the maximum deformation was calculated and used as a parameter indicating elasticity. In this study, these parameters were referred to as the softness parameter R0 and elasticity parameter R7, respectively, and were employed as evaluation indices.

Fabrication of soft-headforms using an elastic material and evaluation of the softness and elasticity parameters

After obtaining data on the softness and elasticity parameters by measuring the subject faces, five types of soft headforms based on the Specified PCA panel for Japanese workers were fabricated. The headform skin layers were fabricated using an elastic silicone rubber-based material (Toughsilon®, Tanac Ltd., Gifu, Japan), which is commonly used in the medical field for artificial skin in surgical training and artificial organs. Figure 3 briefly illustrates the process from the 3D digital model data to the materialization of the soft headform. The soft headform was primarily composed of an outer elastic skin layer and a hard inner core. The 3D digital data of the headform were input to a milling machine, and a resin mold was created for the outer skin layer. The inner core model was designed using 3D computer-aided design (CAD) to ensure that the skin layer at each part of the headform face achieved the target thickness. After modeling, the core model was produced using a 3D printer. The soft headforms were created by placing the inner core model inside the resin mold and casting the elastic material into the gap between them. It should be noted that harder silicone rubber parts were embedded in the nose and ear areas of the headform, as the material used for the skin layer made them too soft. For the five fabricated soft headforms, the softness parameter R0 and the elasticity parameter R7 were measured three times at each facial point using the skin softness and elasticity meter in the same manner as in the subject test.

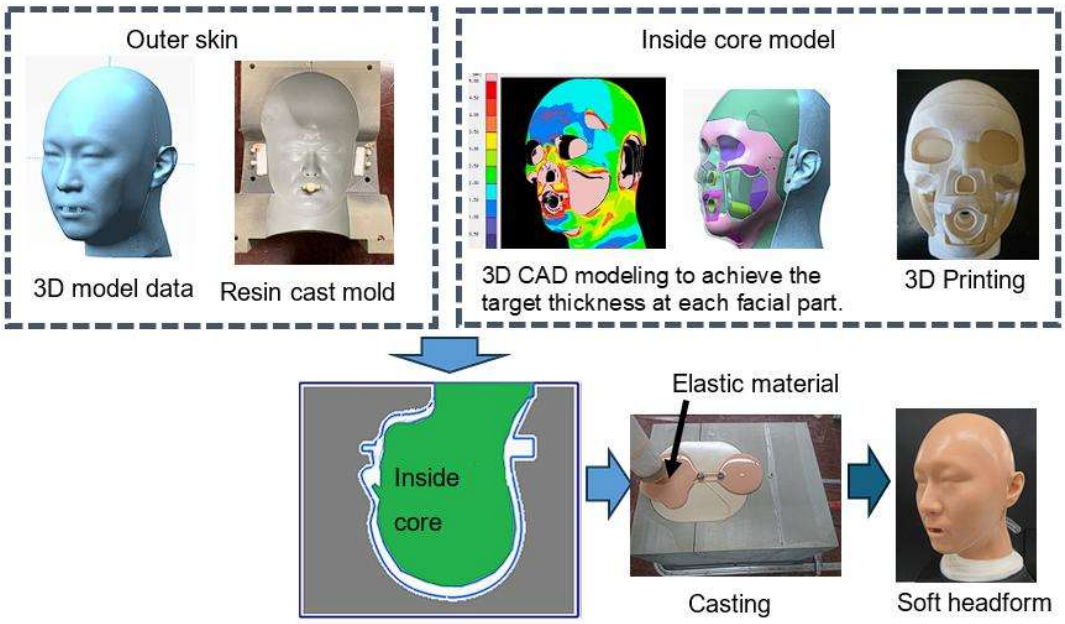


Figure 3. Overview of the process of mold making and fabrication of the soft-headform.

Evaluation of respirator fit of soft headforms

The respirator fit of the soft headforms was evaluated by comparing fit factors with those of hard headforms with identical dimensions and a conventional hard material (plastic) surface. Fit factor measurements were performed using a Mask-fitting Tester MT-05U (Sibata Scientific Technology Ltd., Tokyo, Japan). The fit factor was calculated as the ratio of the ambient particle concentration (>0.3 μm) outside the facepiece to the concentration inside the facepiece when the respirator was donned on the headform. The headforms were connected to a breathing simulator (Koken Ltd., Tokyo, Japan), while a cyclic flow with a sinusoidal waveform of 10 L/min was used as the breathing condition, assuming a static respiratory flow rate. Table I presents six commercially available half-mask respirator models used in this study, certified either under the Japanese national standard for dust masks or by NIOSH under 42 CFR Part 84, coded alphabetically without specifying product names. Given that the filter classes and certified standards differed, a preliminary verification test was conducted. Each respirator model was affixed to a test holder to ensure complete facial sealing. It was subsequently confirmed that the leakage was below the detection limit (zero count) under the same test conditions as in the headform evaluation. Consequently, it has been posited that the particles observed inside the facepiece when deposited on the headform could be attributed to the face seal. Respirators were donned on the headforms according to the manufacturer's instructions, ensuring correct head strap positioning and adjusting the nose clip as needed. Although some respirator models are equipped with fit checkers that allow wearers to perform negative or positive pressure fit checks, headforms cannot perform these checks in the same manner as human wearers. Bergman et al. (2014) previously reported that when evaluating the respirator fit of NIOSH-certified respirators on the advanced headform, they utilized a real-time screening of fit factors with PortaCount Pro+ (TSI Inc., Shoreview, Minnesota., USA) to preliminarily assess the respirator fit and make necessary adjustments. This screening method resulted in high fit factors, comparable to anticipated results when the respirators were worn by wearers. As such, the real-time measurement function, which was also included in the MT-05U, was utilized to don the respirators to the headforms. After donning the respirators onto the headforms and adjusting the respirator position, nose clip, and head straps, the breathing simulator generated the cyclic flow. While monitoring the fit factor values using the real-time measurement function, further adjustments were made to confirm that the respirator fit condition that stably achieved the highest fit factor. After confirming the optimal fit condition, the respirator was temporarily removed and subsequently redonned to replicate the previously confirmed optimal fit as accurately as possible, after which the actual fit factor measurement was conducted. This procedure — donning the respirator, adjusting its position and straps while monitoring fit factor in real-time, removing it, and redonning — was repeated three times by one test operator for each respirator and headform combination.

Table I. Respirator models for fit factor evaluation.

Model	Type	Class	Certification Standard
A	Filtering facepiece	N95/DS2	Japanese Standard [a]
B	Elastomeric half-mask	RL2	
C	Elastomeric half-mask	RL2	
D	Elastomeric half-mask	RL2	
E	Elastomeric half-mask	N95	NIOSH [b]
F	Filtering facepiece	P95	

[a] Japanese national standard for dust masks (Ministry of Health, Labor, and Welfare, 1963)
[b] 42 CFR Part 84 (Code of Federal Register, 1995)

RESULTS AND DISCUSSION

Softness and elasticity parameters on subject face

Table II shows the descriptive statistics for parameters R0 and R7, respectively, which were calculated from the deformation curves at each facial measurement point of the subjects. The mean R0 values varied across the measurement points, ranging from 0.53 (forehead region) to 1.12 (cheek region 3) while mean R7 values were relatively consistent ranging from 0.42 to 0.49. To observe statistically significant differences in R0, a Friedman test was conducted, which revealed significant differences among measurement points ($p<0.01$). A Scheffé post-hoc test was then conducted to classify the measurement points. Among them, the forehead region exhibited the lowest mean R0 value. Compared to the forehead, no significant differences in R0 were found for the frontotemporal region, zygion, glabella, cheek region 1, and chin ($p>0.05$ for all). In contrast, significant differences were found for the nose side and gonion (both $p<0.05$), as well as for cheek regions 2 and 3 ($p<0.01$), which showed higher mean R0 values than the forehead. For R7, the same analysis revealed no significant differences across any of the measurement points. Based on these findings, the facial measurement points were roughly grouped into three categories, as shown in Table III, and corresponding target value ranges were defined for soft headform fabrication. The target value ranges for the relatively firm and soft categories were determined based on rounded values derived from the lowest and highest mean R0 values ± standard deviations within each group. Specifically, the relatively firm category was defined as ranging from 0.4 to 0.7, based on values at the forehead and cheek region 1. The soft category was defined as ranging from 0.8 to 1.3, based on cheek regions 2 and 3. The target range for the relatively soft category was set to begin at 0.7, the upper limit of the relatively firm group, to clearly distinguish it from the firm category and the upper limit, 1.0, was based on the value observed at the gonion. The target range for R7 was uniformly set to 0.4 to 0.6 across all categories, based on values at the glabella and cheek region 2. These simplified category classifications and target values ranges were used as references in the actual fabrication of the headforms.

Table II. Descriptive statistics for parameters R0 and R7 on 10 measurement points obtained from subject faces (n=31).

	R0					R7				
Measurement point	Mean (SD)	Min	Max	95% CI (Lower)	95% CI (Upper)	Mean (SD)	Min	Max	95% CI (Lower)	95% CI (Upper)
a. Forehead region	0.53 (0.15)	0.30	0.92	0.47	0.58	0.44 (0.05)	0.31	0.55	0.42	0.46
b. Frontotemporal region	0.54 (0.14)	0.27	0.82	0.47	0.58	0.44 (0.06)	0.28	0.59	0.42	0.46
c. Zygion	0.60 (0.13)	0.37	0.89	0.55	0.64	0.44 (0.07)	0.29	0.61	0.42	0.47
d. Gonion	0.76 (0.23)	0.36	1.38	0.67	0.84	0.47 (009)	0.31	0.70	0.44	0.50
e. Glabella	0.59 (0.14)	0.35	0.87	0.54	0.64	0.42 (0.07)	0.28	0.59	0.40	0.45
f. Nose side region	0.76 (0.19)	0.26	1.07	0.69	0.83	0.48 (0.05)	0.37	0.57	0.47	0.50
g. Cheek region 1	0.62 (0.12)	0.41	0.89	0.57	0.66	0.44 (0.07)	0.30	0.59	0.41	0.47
h. Cheek region 2	0.93 (0.18)	0.67	1.33	0.87	1.00	0.49 (0.07)	0.34	0.65	0.46	0.51
i. Cheek region 3	1.12 (0.17)	0.81	1.56	1.05	1.18	0.49 (0.06)	0.36	0.58	0.47	0.51
j. Chin	0.56 (0.10)	0.40	0.77	0.53	0.60	0.45 (0.07)	0.34	0.62	0.43	0.48

Table III. Target R0 and R7 values based on measurement of subject faces.

Measurement point	Category	R0	R7
a, b, c, e, g, j	Relatively firm	0.4 - 0.7	0.4 - 0.6
d, f	Relatively soft	0.7 - 1.0	
h, i	Soft	0.8 - 1.3	

Fabrication of soft headforms using the elastic material

Figure 4 presents the deformation curves of the test plate pieces with different thicknesses of the elastic material used for the soft headform. Parameter R0, which represents the maximum deformation displacement during decompression, varied depending on the thickness of the test piece. For parameter R7, the values remained at approximately 0.5, irrespective of the thickness. Thus, by adjusting the thickness of the elastic material in each region of the headform face, the target R0 value can be approached. The thickness of the elastic material in the soft headform was determined by the gap distance between the outer mold and the inner core model. The inner core model was designed in 3D CAD, utilizing the relationship between the thickness of the test piece and R0 values as a reference (e.g., a thickness of approximately 2 mm in relatively firm regions). However, the R0 values of the headform faces after casting the elastic material often departed from the set range, requiring trial-and-error adjustments to the thickness by applying putty or sanding the inner core model. As such, the exact thickness of the elastic material in each facial region of the soft headform could not be determined. Figure 5 presents the five fabricated soft headforms with varying facial sizes and shapes. Nylon tubes were affixed to the mouth and both nostrils to facilitate connection to a breathing simulator and enable particle sampling within the facepiece.

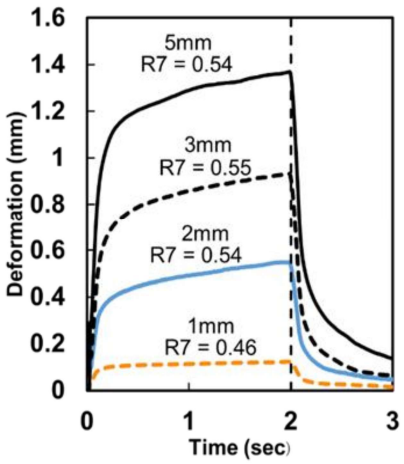


Figure 4. Deformation curves of different thicknesses of the material used for the soft headforms.



Figure 5. Five soft headforms representing the medium, and four facial categories based on the specified PCA panel, for Japanese workers.
(from left to right: Medium, Small, Large, Short-Wide, and Long-Narrow)

Table IV presents the mean and standard deviations of the parameters R0 and R7 derived from the deformation curves of the facial measurement points of each soft headform, along with the predetermined target value ranges for the corresponding categories based on the subject test. In this table, bold text indicates that the mean R0 and R7 values at the given facial measurement point fall outside the corresponding target value ranges. For R0, three points — zygion and cheek regions 2 and 3 — on the Small type soft headform were found to have mean values outside the target ranges. For the Large type, cheek regions 2 and 3 also showed mean values outside the ranges. Regarding R7, only the glabella point on the Small type had a mean value outside the target range, whereas all other points on all soft headform types were confirmed to fall within the target ranges. Additionally, the conformity of the mean R0 and R7 values at each facial measurement point on each soft headform to the predefined target range was statistically evaluated using one-sample t-tests, which compared each mean value to the lower and upper bounds of the range. The results are presented in Table V. The p-values for comparisons with the lower and upper bounds are denoted by p(L) and p(U), respectively. For example, in the results for the Small type headform, the target R0 range for the forehead region, which was classified under the relatively firm category, was set between 0.4 and 0.7. The mean R0 value at the forehead region of the Small type was 0.62, which was within the target range. Since statistically significant differences ($p<0.05$) were detected when this mean was compared to both the lower (0.4) and upper (0.7) bounds using one-sample t-tests, the mean value was judged to be within the target range ($0.4 < \text{Mean R0} < 0.7$). In contrast, at the zygion, the mean R0 value was 0.81, which exceeds the upper bound of the target range (0.7). Since a statistically significant difference ($p<0.05$) was also detected when compared to the upper bound, the mean R0 was judged to be significantly greater than the upper bound ($\text{Mean R0} > 0.7$), indicating that it was substantially outside the target range. Similarly, at cheek region 2, the mean R0 value was 1.34, which exceeds the upper bound of the target range (1.3). However, since no statistically significant difference was detected in comparison with the upper bound ($p>0.05$), the mean was judged to be only slightly outside the target range. Furthermore, as another example, at the Frontotemporal region of the Medium type, the mean R0 value was 0.65, which falls within the target range of 0.4 to 0.7. However, since the result was not significantly lower than the upper bound of 0.7($p>0.05$), the mean was also judged to be slightly outside the target range. Based on these criteria, as shown in the table, the mean R0 values for the Small type were found to be substantially outside the target range at one measurement point (zygion) and slightly outside at two points (cheek regions 2 and 3), whereas the values at the remaining points were confirmed to fall within the target range. Similarly, for the Medium type, the mean R0 values were slightly outside the target range at two measurement points (frontotemporal region and gonion)； Large type, at three points (glabella and cheek regions 2 and 3); Short-Wide type, at four points (gonion, cheek regions 2 & 3, and chin); and Long-Narrow type, at one point (cheek region 3). At all other measurement points, the mean R0 values were confirmed within the target range. At the points where the values were outside the target range, the thickness adjustment of the elastic material achieved by modifying the inner core model was deemed inadequate. For R7, slightly outside values were observed only at two points (glabella and chin) on the Small type, one point (chin) on the Large type, and one point (chin) on the Long-Narrow type. Since these deviations were concentrated at a specific location (chin), possible causes may include the inclusion of air

bubbles or mold release agent in the elastic material during casting; however, the exact reason remains unclear.

Table IV. Parameters R0 and R7 for 10 facial measurement points on each soft headform (Mean ± SD). Bold values indicate that the mean falls outside the predefined target range for the corresponding categories.

Measurement point	Parameter	Target value range	Mean R0(SD) and R7(SD)				
			Small	Medium	Large	Short-Wide	Long-Narrow
a. Forehead region	R0	0.4-0.7	0.62(0.02)	0.54(0.07)	0.52(0.03)	0.56(0.08)	0.53(0.03)
	R7	0.4-0.6	0.45(0.02)	0.53(0.04)	0.53(0.04)	0.48(0.04)	0.51(0.03)
b. Frontotemporal region	R0	0.4-0.7	0.59(0.06)	0.65(0.10)	0.56(0.06)	0.57(0.05)	0.59(0.06)
	R7	0.4-0.6	0.45(0.03)	0.51(0.04)	0.47(0.04)	0.46(0.02)	0.48(0.04)
c. Zygion	R0	0.4-0.7	**0.81(0.05)**	0.53(0.05)	0.54(0.04)	0.58(0.04)	0.58(0.05)
	R7	0.4-0.6	0.52(0.05)	0.47(0.04)	0.49(0.04)	0.54(0.03)	0.50(0.03)
d. Gonion	R0	0.7-1.0	0.93(0.03)	0.74(0.05)	0.79(0.05)	0.71(0.08)	0.81(0.06)
	R7	0.4-0.6	0.47(0.01)	0.51(0.05)	0.50(0.03)	0.49(0.01)	0.47(0.04)
e. Glabella	R0	0.4-0.7	0.51(0.04)	0.62(0.06)	0.61(0.11)	0.61(0.04)	0.58(0.06)
	R7	0.4-0.6	**0.39(0.07)**	0.50(0.05)	0.49(0.01)	0.48(0.03)	0.47(0.04)
f. Nose side region	R0	0.7-1.0	0.89(0.02)	0.92(0.02)	0.74(0.02)	0.79(0.05)	0.74(0.02)
	R7	0.4-0.6	0.51(0.05)	0.54(0.03)	0.51(0.02)	0.51(0.05)	0.51(0.05)
g. Cheek region 1	R0	0.4-0.7	0.65(0.03)	0.59(0.04)	0.53(0.07)	0.54(0.07)	0.55(0.08)
	R7	0.4-0.6	0.46(0.03)	0.54(0.02)	0.43(0.01)	0.47(0.04)	0.50(0.05)
h. Cheek region 2	R0	0.8-1.3	**1.34(0.24)**	1.11(0.05)	**1.37(0.11)**	1.27(0.12)	1.10(0.13)
	R7	0.4-0.6	0.54(0.03)	0.56(0.02)	0.52(0.03)	0.51(0.03)	0.49(0.03)
i. Cheek region 3	R0	0.8-1.3	**1.33(0.20)**	1.16(0.07)	**1.36(0.15)**	1.23(0.08)	1.12(0.14)
	R7	0.4-0.7	0.53(0.03)	0.55(0.01)	0.55(0.03)	0.49(0.03)	0.50(0.04)
j. Chin	R0	0.4-0.7	0.56(0.07)	0.65(0.04)	0.61(0.05)	0.69(0.05)	0.65(0.02)
	R7	0.4-0.6	0.41(0.02)	0.48(0.02)	0.41(0.04)	0.43(0.01)	0.42(0.03)

Table V. Result of p-values from one-sample t-tests comparing mean R0 and R7 values at each facial measurement point to the lower [p(L)] and upper [p(U)] bounds of the target range.

Measurement point	Parameter	Small		Medium		Large		Short-Wide		Long-Narrow	
		p(L)	p(U)	p(L)	p(U)	p(L)	p(U)	p(L)	p(U)	p(L)	p(U)
a. Forehead region	R0	0.001	0.010	0.003	0.030	0.007	0.003	0.032	0.044	0.009	0.006
	R7	0.025	0.003	0.012	0.034	0.017	0.046	0.036	0.015	0.001	0.004
b. Frontotemporal region	R0	0.001	0.004	0.023	**0.217^{C}**	0.025	0.032	0.014	0.021	0.018	0.043
	R7	0.047	0.007	0.024	0.030	0.039	0.012	0.021	0.003	0.041	0.023
c. Zygion	R0	0.005	**0.027^{A}**	0.023	0.014	0.011	0.008	0.009	0.019	0.014	0.027
	R7	0.023	0.049	0.044	0.016	0.025	0.020	0.013	0.038	0.011	0.010
d. Gonion	R0	0.002	0.019	**0.134^{C}**	0.006	0.043	0.008	**0.473^{C}**	0.011	0.037	0.015
	R7	0.005	0.001	0.035	0.044	0.010	0.011	0.003	0.002	0.009	0.002
e. Glabella	R0	0.020	0.006	0.002	0.012	0.043	**0.152^{C}**	0.005	0.022	0.021	0.040
	R7	**0.438^{B}**	0.016	0.041	0.037	0.001	0.000	0.023	0.013	0.042	0.012
f. Nose side region	R0	0.002	0.004	0.026	0.013	0.020	0.001	0.043	0.008	0.035	0.001
	R7	0.035	0.044	0.008	0.033	0.003	0.004	0.027	0.035	0.033	0.042
g. Cheek region 1	R0	0.002	0.041	0.009	0.000	0.042	0.026	0.031	0.026	0.045	0.041
	R7	0.030	0.005	0.003	0.021	0.018	0.000	0.044	0.016	0.036	0.032
h. Cheek region 2	R0	0.031	**0.401^{B}**	0.005	0.013	0.006	**0.202^{B}**	0.008	**0.373^{C}**	0.028	0.039
	R7	0.008	0.035	0.003	0.035	0.007	0.017	0.016	0.022	0.012	0.009
i. Cheek region 3	R0	0.023	**0.423^{B}**	0.006	0.037	0.011	**0.273^{B}**	0.004	**0.123^{C}**	0.027	**0.076^{C}**
	R7	0.010	0.029	0.001	0.007	0.005	0.044	0.012	0.009	0.019	0.019
j. Chin	R0	0.031	0.041	0.022	0.067	0.010	0.044	0.004	**0.354^{C}**	0.002	0.031
	R7	**0.309^{C}**	0.003	0.015	0.007	**0.401^{C}**	0.007	0.028	0.003	**0.183^{C}**	0.005

Bold values and superscript letters indicate the following:
A: The mean is outside the target range and shows a statistically significant difference from either the lower or upper bound.
B: The mean is outside the target range but does not show a statistically significant difference from either the lower or upper bound.
C: The mean is within the target range and does not show a statistically significant difference from either the lower or upper bound.

Respirator fit evaluation of soft headforms

Table VI presents the geometric mean fit factors (GM FF) and geometric standard deviations for both soft and corresponding hard headforms across the six respirator models. Aggregated data for all respirator models have also been included to offer a comprehensive overview of the overall trends. As fit factors typically follow a log-normal distribution, previous studies (Groce et al., 2010; Bargman et al., 2014) utilized logarithmic transformation for analysis. Following this approach, we also log-transformed the fit factor data and used Welch's t-test to assess differences between the soft and hard headforms; the results are summarized in the table. The respirator models used in this study were certified either under the Japanese national standard for dust masks or by NIOSH under 42 CFR Part 84; thus, achieving a fit factor >100 could be anticipated when worn by actual wearers.

All 30 combinations (six respirator models × five headform types) with hard headforms had GM FF values

<100. In contrast, 17 out of the 30 combinations with soft headforms exceeded a GM FF of 100. Furthermore, except for the Small and the Short-Wide types with respirator model E, all combinations demonstrated significantly higher fit factors for the soft headforms compared to the corresponding hard headforms. This result was attributed to the elastic material used for the soft headforms, which effectively improved respirator fit.

Table VI. Geometric mean fit factor (GM FF) for hard and soft headforms by respirator models. Values in parentheses indicate geometric standard deviation (GSD).

Respirator model	Material	Small	Medium	Large	Short-Wide	Long-Narrow
A	Hard	29 (1.1)	29 (1.0)	15 (1.2)	55 (1.1)	16 (1.1)
	Soft	160 (1.2)**	316 (1.6)*	114 (1.3)**	270 (1.3)**	50 (1.3)**
B	Hard	14 (1.1)	44 (1.2)	17 (1.0)	10 (1.1)	31 (1.1)
	Soft	63 (1.3)**	291 (1.6)*	686 (2.3)*	119 (1.1)**	401 (1.6)**
C	Hard	8 (1.1)	22 (1.1)	15 (1.1)	8 (1.1)	29 (1.1)
	Soft	39 (1.0)**	128 (1.1)**	120 (1.6)*	70 (1.4)**	179 (1.3)**
D	Hard	7 (1.2)	31 (1.1)	20 (1.1)	16 (1.0)	17 (1.1)
	Soft	80 (1.3)**	184 (1.6)*	111 (1.2)**	252 (2.4)*	109 (1.5)*
E	Hard	5 (1.2)	3 (1.1)*	4 (1.0)	15 (1.1)	3 (1.1)
	Soft	13 (1.6)	27 (1.9)*	17 (1.1)**	28 (1.4)	7 (1.1)**
F	Hard	5 (1.1)	27 (1.0)	11 (1.0)	11 (1.4)	15 (1.1)
	Soft	16 (1.2)**	86 (1.4)*	118 (1.2)**	73 (1.2)**	101 (1.3)**
Total	Hard	9 (1.9)	21 (2.4)	12 (1.7)	15 (2.0)	14 (2.3)
	Soft	43 (2.5)**	131 (2.6)**	113 (3.2)**	102 (2.4)**	81 (3.7)**

* p<0.05 ** p<0.01

Additionally, among the five headform types, the Medium type was designed as the reference shape, while the other four were designed to reflect differences in facial features such as size, contours, nose, and cheek shapes. Therefore, to examine the differences in fit factors relative to the Medium type, Kruskal–Wallis tests and Shirley–Williams multiple comparisons were conducted separately by material type using log-transformed fit factors. The results are listed in Table VII.

From the Kruskal–Wallis tests, significant differences were detected in all combinations for the hard headforms, with p<0.05 for respirator models A, C, D, and F, and p<0.01 for models B and E. In contrast, for the soft headforms, significant differences (p<0.05) were found for models A, B, C, E, and F, whereas no significant difference was observed for model D. In the Shirley–Williams multiple comparisons using the Medium type as the reference, for the respirator model A, a significant difference was observed only in the Large type for the hard headforms, while significant differences were found in three types: Long-Narrow, Large, and Small for the soft headforms. However, for the remaining five respirator models, significant differences in the hard headforms were observed in three types (Short-Wide, Large, Small), or in four types when the Long-Narrow was additionally included. For the soft headforms, significant differences were observed only in one type, either Small or Long-Narrow. These results suggest that the soft headforms, which can deform to an extent in response to the respirator facepiece shape, may have mitigated differences in fitting, whereas the hard headforms, with their rigid and non-deformable facial surfaces, exhibited more prominent differences in the fitting between the face and facepiece due to variations in facial features. Given that the headforms were modeled in accordance with the facial size and shape categories defined in the Specified PCA panel for Japanese workers, future comparative studies involving human subjects categorized within the same facial size and shape groups may provide additional insights into the effects of headform material and facial features on respirator fit.

Table VII. Results of Kruskal–Wallis tests and Shirley–Williams multiple comparisons for differences in fit factor among headform shapes (Medium as reference).

Respirator model	Material	Kruskal–Wallis p-value	Headform Comparison (Medium vs.)	Direction	Shirley–Williams Multiple Comparisons Test statics	5% critical value	2.5% critical value	Significance
A	Hard	0.016	Large	Medium>	2.236	1.716	2.015	**
	Soft	0.014	Long-Narrow	Medium>	2.921	1.750	2.040	**
			Large	Medium>	2.534	1.716	2.015	**
			Small	Medium>	1.964	1.645	1.960	**
B	Hard	0.009	Long-Narrow	Medium>	2.054	1.750	2.040	**
			Short-Wide	Medium>	3.057	1.739	2.032	**
			Large	Medium>	2.012	1.716	2.015	*
			Small	Medium>	1.964	1.645	1.960	**
	Soft	0.020	Small	Medium>	1.964	1.645	1.960	**
C	Hard	0.012	Short-Wide	Medium>	2.491	1.739	2.032	**
			Large	Medium>	2.012	1.716	2.015	*
			Small	Medium>	1.964	1.645	1.960	**
	Soft	0.024	Small	Medium>	1.964	1.645	1.960	**
D	Hard	0.012	Long-Narrow	Medium>	2.100	1.750	2.040	**
			Short-Wide	Medium>	2.038	1.739	2.032	**
			Large	Medium>	2.012	1.716	2.015	*
			Small	Medium>	1.964	1.645	1.960	**
	Soft	0.097	Small	Medium>	1.964	1.645	1.960	**
E	Hard	0.009	Short-Wide	Medium<	3.057	1.739	2.032	**
			Large	Medium<	2.012	1.716	2.015	*
			Small	Medium<	1.964	1.645	1.960	**
	Soft	0.036	Long-Narrow	Medium>	2.556	1.750	2.040	**
F	Hard	0.014	Long-Narrow	Medium>	2.054	1.750	2.040	**
			Short-Wide	Medium>	2.038	1.739	2.032	**
			Large	Medium>	2.012	1.716	2.015	*
			Small	Medium>	1.964	1.645	1.960	**
	Soft	0.0410	Small	Medium>	1.964	1.645	1.960	**
Total	Hard	0.0021	Long-Narrow	Medium>	2.632	1.750	2.04	**
			Short-Wide	Medium>	2.771	1.739	2.032	**
			Large	Medium>	3.115	1.716	2.015	**
			Small	Medium>	2.816	1.645	1.96	**
	Soft	0.0173	Large	Medium>	1.939	1.716	2.02	*
			Small	Medium>	3.101	1.645	1.96	**

Note: This table shows only headform types with significant differences.
* indicates that the test statistic exceeded the 5% critical value; ** indicates that the test statistic exceeded the 2.5% critical value

Study limitations

In the present study, the skin deformation data at each facial point were obtained from a limited number of subjects (n = 31). Although classification based on the previously defined PCA panel confirmed that all facial categories were represented, in this study, the skin deformation data (R0 and R7) were calculated without classifying subjects by facial category. Consequently, the calculated skin deformation data represent general trends across the overall sample and may not capture the specific characteristics of each facial category. This limitation should be considered when interpreting the representativeness and applicability of the soft headforms. In addition, the number of repeated measurements for R0 and R7 at each facial point on the soft headforms was limited to three (n = 3), which may limit the statistical power of the one-sample t-tests used to assess conformity with the target ranges. Although additional measurements could not be conducted during the course of this study, increasing the number of repetitions should be considered in future studies or similar efforts. Moreover, respirators were donned and re-donned onto headforms to achieve an optimal fit, which was monitored in advance using the real-time measurement

function of the device. As this redonning was conducted by a single experienced operator, different results may have been obtained if performed by different operators. Additionally, given that only six respirator models were used, different respirator models may have yielded different results. Furthermore, the elastic material used for the headforms is a silicone rubber-based material, and the electrostatic charge of the material may influence the particle behavior in the facepiece.

CONCLUSIONS

This study aimed to develop and evaluate soft headforms based on Japanese facial features with the goal of improving the accuracy of respirator fit testing. Soft headforms based on five 3D digital models derived from the Specified Japanese PCA panel were fabricated using an elastic material. Using one-sample t-tests, the most of the softness parameter (R0) and the elasticity parameter (R7) for each facial point of the fabricated soft headforms fell within the target value ranges set as a reference based on the results of the subject test. A comparative evaluation of the respirator fit of the soft headforms with commercially available respirator models and hard headforms of identical dimensions demonstrated that the soft headforms exhibited higher fit factors in most respirator model/headform type combinations, confirming the effectiveness of the elastic material in enhancing respirator fit. Furthermore, using the Medium type as the reference, differences in fit factors among the other four headform types representing variations in facial features were analyzed using the Kruskal–Wallis and Shirley–Williams tests. As a result, significant differences between the Medium type and the other headform types were detected less frequently in the soft headforms than in the hard headforms. This result suggests that their deformable surfaces may help reduce the impact of facial shape variation on respirator fit.

The ultimate goal is to establish soft headforms as reliable surrogates for human subjects in respirator fit testing. To achieve this, further research is necessary to validate whether the fit factors obtained using these soft headforms correspond closely with those measured on actual Japanese workers. Specifically, it is essential to conduct comparative testing between the soft headforms and human subject groups representing the facial categories defined in the panel, and to determine whether there is a significant correlation in fit performance. Such findings would provide strong evidence that the soft headforms can serve as superior substitutes for traditional hard headforms in fit testing protocol.

REFERENCES

Akhtar N, Zaman SU, Khan BA, Amir MN, Ebrahimzadeh MA. (2011) Calendula extract: effects on mechanical parameters of human skin. *Acta Pol. Pharm*. 68(5): 693-701.

Bergman MS, Zhuang Z, Hanson D, Heimbuch BK, McDonald MJ, Palmiero AJ, Shaffer RE, Harnish D, Husband M, Wander JD. (2014). Development of an advanced respirator fit-test headform. *J. Occup. Environ. Hyg*. 11: 117-125.

Bergman MS, He X, Joseph ME, Zhuang Z, Heimbuch BK, Shaffer RE, Choe M, Wander JD. (2015) Correlation of respirator fit measured on human subjects and a static advanced headform. *J. Occup. Environ. Hyg.* 12: 163-171.

Code of Federal Regulations (1995). Respiratory protective device: Final rules and notice. U.S. Government Printing Office of Federal Register, Washington, DC. Title 42, Part 84.

Cooper DW, Hinds WC, Price JM, Weker R, Yee HS. (1983) Common materials for emergency respiratory protection: leakage tests with a manikin. *Am. Ind. Hyg. Assoc.J.* 44: 720–726.

Courage + Khazaka electronic GmbH. Abstracts Cutometer (Updated on 16 July 2024). https://www.courage-khazaka.com/en/downloads-en/category/study-lists.

Golshahi L, Telidetzki K, King B, Shaw D, Finlay WH. (2013) A pilot study on the use of geometrically accurate face models to replicate ex vivo N95 mask fit. *Am. J. Infect. Control*. 41: 77-79.

Groce G, Guffey S, Viscusi DJ, Lynch S, Benson S, Zhuang Z. (2010) Three-dimensional facial parameters and principal component scores: Association with respirator fit. *J. Int. Soc. Respir. Prot.* 27: 1-14.

Grinshpun SA, Haruta H, Eninger RM, Reponen T, McKay RT, Lee SA. (2009) Performance of an N95 filtering facepiece particulate respirator and a surgical mask during human breathing: two pathways for particle penetration. *J. Occup. Environ. Hyg.* 6: 593-603.

Hack A, Hyatt EC, Held BJ, Moore TO, Richards CP, McConville JT. (1974) Selection of respirator test

panels representative of U.S. adult facial sizes. https://doi.org/10.2172/4335046
Haruta H, Yuasa H, Shimizu E, Koyama T, Kimura K. (2016) Survey on face size of Japanese workers for evaluating respirator fit. *Journal of ISRP Japan Section Respiratory Protection*. 28(2): 2-8.
Haruta H. (2023) 3D modeling of headforms representing Japanese facial features for adequate fit testing. *Journal of ISRP Japan Section Respiratory Protection*. 55: 2-8.
He X, Grinshpun SA, Reponen T, McKay RT, Bergman MS, Zhuang Z. (2014) Effects of breathing frequency and flow rate on the total inward leakage of an elastomeric half-mask donned on an advanced manikin headform. *Ann. Occup. Hyg*. 58(2): 182-194.
Hinds WC, Kraske G. (1987) Performance of dust respirators with facial seal leaks: I. Experimental. *Am. Ind. Hyg. Assoc. J.* 48(10): 836–841.
Instruction Manual MPA580 (2013). Courage + Khazaka electronic GmbH., Cologne: 25-26.
International Organization for Standardization. (2022) Respiratory protective devices – Human factors. Part2: Anthropometrics. ISO/TS 16976-2:2022, Geneva: International Organization for Standardization: 13.
Joe PS, Floyd EL, Lungu CT. (2012). Physical fabrication and verification of new NIOSH digital headform designs with skin-analog for use in fit testing. *J. Int. Soc. Respir. Prot.* 29(2): 82-93.
Kawabata M, Yabuzaki J, Yamakawa Y, Oba A. (2012) Sphere-drop test: New visualization method for assessing mechanical properties of skin with tactile elements-softness and elasticity. *J. Soc. Cosmet. Chem. Jpn.* 46(3): 205-218.
Krishnan U, Willeke K, Juozaitis A, Myojo T, Talaska G, Shukla R. (1994) Variation in quantitative respirator fit factors due to fluctuations in leak size during fit testing. *Am. Ind. Hyg. Assoc. J.* 55(4):309-314.
Lee AL, Cui X, Jung H, Kim, HE, Jeon E J, Na H, Kim E, You H. (2024) Development of Korean representative headforms for the total inward leakage testing on filtering facepiece respirators. *Saf. Health. Work*. 15(1): 42-52.
Ministry of Health, Labor, and Welfare. (1963). Standards for dust masks: Ministerial notification No.19. Accessed October 19, 2024. https://www.mhlw.go.jp/web/t_doc?dataId=74041000
Ministry of Health, Labor, and Welfare. (2016). Standards for respirators with electric fans: Ministerial notification No. 455. Accessed October 19, 2024.
Myers WR. (2000) Ch 32: Respiratory protective equipment. In: Patty's Industrial Hygiene. 5th ed. pp 1501-1505. Harris RL, ed New York: John Wiley & Sons, Inc.
Oestenstad RK, Dillion HK, Perkins LL. (1990) Distribution of faceseal leak sites on a half-mask respirator and their association with facial dimensions. *Am. Ind. Hyg. Assoc. J.* 51: 285-290.
Rengasamy S, Eimer BC. (2011) Total inward leakage of nanoparticles through filtering facepiece respirators. *Ann. Occup. Hyg.* 55(3):253-263.
Tuomi T. (1985) Face seal leakage of half-masks and surgical masks. *Ame. Ind. Hyg. Assoc. J.* 46:308–312.
Yu Y, Benson S, Cheng W, Hsiao J, Liu Y, Zhuang Z, Chen W. (2012) Digital 3-d headforms representative of Chinese workers. *Ann. Occup. Hyg.* 56(1): 113-122.
Zhuang, Z., Benson, S., Viscusi, D. (2010) Digital 3-D headforms with facial features representative of the current US workforce. *Ergonomics*. 53(5): 661-671.
Zhuang Z, Bradmiller B. (2005) Head-and-face anthropometric survey of U.S. respirator users. *J. Occup. Environ. Hyg.* 2:567-576.
Zhuang Z, Bradmiller B, Shaffer RE. (2007) New respirator fit test panels representing the current U.S. civilian work force. *J. Occup. Environ. Hyg.* 4:647-659.